Atmospheric pressure chemical ionization of fluorinated phenols in atmospheric pressure chemical ionization mass spectrometry, tandem mass spectrometry, and ion mobility spectromet...

5 AUTHORS, INCLUDING:

Zeev Karpas

3QBD Ltd

96 PUBLICATIONS **1,711** CITATIONS

SEE PROFILE

Atmospheric Pressure Chemical Ionization of Fluorinated Phenols in Atmospheric Pressure Chemical Ionization Mass Spectrometry, Tandem Mass Spectrometry, and Ion Mobility Spectrometry

G. A. Eiceman, J. F. Bergloff, J. E. Rodriguez, W. Munro,[†] and
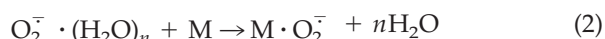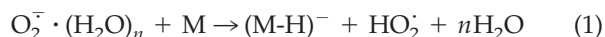Z. Karpas[‡]
Department of Chemistry and Biochemistry, New Mexico State University, Las Cruces, New Mexico, USA

Atmospheric pressure chemical ionization (APCI)-mass spectrometry (MS) for fluorinated phenols ($C_6H_{5-x}F_xOH$ where $x = 0$–5) in nitrogen with Cl^- as the reagent ion yielded product ions of $M \cdot Cl^-$ through ion associations or $(M - H)^-$ through proton abstractions. Proton abstraction was controllable by potentials on the orifice and first lens, suggesting that some proton abstraction occurs through collision induced dissociation (CID) in the interface region. This was proven using CID of adduct ions ($M \cdot Cl^-$) with Q2 studies where adduct ions were dissociated to Cl^- or proton abstracted to $(M - H)^-$. The extent of proton abstraction depended upon ion energy and structure in order of calculated acidities: pentafluorophenol > tetrafluorophenol > trifluorophenol > difluorophenol. Little or no proton abstraction occurred for fluorophenol, phenol, or benzyl alcohol analogs. Ion mobility spectrometry was used to determine if proton abstraction reactions passed through an adduct intermediate with thermalized ions and mobility spectra for all chemicals were obtained from 25 to 200 °C. Proton abstraction from $M \cdot Cl^-$ was not observed at any temperature for phenol, monofluorophenol, or difluorophenol. Mobility spectra for trifluorophenol revealed the kinetic transformations to $(M - H)^-$ either from $M \cdot Cl^-$ or from $M_2 \cdot Cl^-$ directly. Proton abstraction was the predominant reaction for tetra- and penta-fluorophenols. Consequently, the evidence suggests that proton abstraction occurs from an adduct ion where the reaction barrier is reduced with increasing acidity of the O–H bond in $C_6H_{5-x}F_xOH$.   (J Am Soc Mass Spectrom 1999, 10, 1157–1165)   © 1999 American Society for Mass Spectrometry

G as phase reactions of negative ions were recognized early in the development of atmospheric pressure chemical ionization (APCI)-mass spectrometry (MS) and in an allied technology, ion mobility spectrometry (IMS) [1–6]. On the whole, such reactions have been considered highly selective and lacking in the broad reactivity or importance recognized for positive ion reactions. Consequently, the reaction pathways for negative ions at ambient pressure have received comparatively little attention even though such reactions are central in certain compelling applications such as monitoring chemical warfare agents [7] and detecting explosives [8, 9]. Despite these uses, our understanding is relatively limited regarding the factors that govern the qualitative and quantitative response in methods based on negative APCI techniques [10–12].

In ionization sources such as corona discharges or β^- emitters, the major reactant ion in clean air at ambient pressure is $O_2^- \cdot (H_2O)_n$ where the value for n is dependent upon temperature and moisture. When a molecule is present in the ion source, reactions may occur through one or more of several reactions including proton abstraction (eq 1), association (eq 2), and charge exchange (eq 3).

$$O_2^- \cdot (H_2O)_n + M \rightarrow (M\text{-}H)^- + HO_2^- + nH_2O \qquad (1)$$

$$O_2^- \cdot (H_2O)_n + M \rightarrow M \cdot O_2^- + nH_2O \qquad (2)$$

$$O_2^- \cdot (H_2O)_n + M \rightarrow M^- + O_2 + nH_2O \qquad (3)$$

Further association (or clustering) reactions may also occur between ions produced in eqs 1–3 and additional neutral molecules leading to dimer ions of the type $M \cdot (M - H)^-$ as shown in eq 4.

Address reprint requests to G. A. Eiceman, Dept. of Chemistry and Biochemistry, New Mexico State University, MSC 3C, Las Cruces, NM 88004. E-mail: geiceman@nmsu.edu
[†] Permanent address: Graseby Ionics, Ltd. Watford, UK.
[‡] Permanent address: Analytical Chemistry Department, Nuclear Research Center, Negev, P. O. Box 9001, Beer-Sheva, Israel 84190.

$$(M - H)^- + M \rightarrow M \cdot (M - H)^- \qquad (4)$$
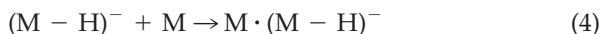
In addition to $O_2^- \cdot (H_2O)_n$, several other reactant ions such as $O_2 \cdot CO_2^-$ and Cl^- may exist in air and some may be associated with trace gas impurities; such mixtures, whether managed or not, will complicate studies on ion molecule chemistry. This can be remedied through the addition of a reagent gas to the ion source to create an alternate reactant ion and simplified ionization chemistry [13]. For example, a chloride reactant ion (Cl^-) can concentrate all prospective product ions for a sample in a single ion, $M \cdot Cl^-$, thus improving the detection limits (e.g., of ethylene glycol dinitrate [14]). Such alternative reagent ions can undergo reactions analogous to those shown in eqs 1–4; for example, Cl^- is known to abstract protons from nitrotoluenes [15] and Cl^- forms adduct ions with phenol [16].

The pathway leading to proton abstraction with Cl^- as the reagent ion may be expected to begin with an association reaction as shown in eq 5 where values of heats of formation (ΔH_f°) for $M \cdot Cl^-$ with phenol and fluorophenol are -109 and -117 kJ mole^{-1}, respectively [17].

$$Cl^- + M \leftrightarrow M \cdot Cl^- \qquad (5)$$

Comparable ΔH_f° values should be anticipated for other fluorine substituted phenols although exact comparisons were not possible owing to missing reference values. Proton abstraction should have an activation barrier and ΔH_f° for $(M - H)^-$ can be expected to vary for individual fluorinated phenols. Reference values were available to calculate ΔH_f° for proton abstraction (kJ mole^{-1}) per eq 6 and were benzyl alcohol, $+159.7$; phenol, $+74$; and pentafluorophenol, -26.

$$M \cdot Cl^- \rightarrow (M - H)^- + HCl \qquad (6)$$

Recently, the proton abstraction from phenol was experimentally determined [18] as 75 ± 13 kJ mole^{-1} which agrees with the calculated value.

The known or calculated acidities (as solution pK_a values) for fluorinated phenols [19] are: phenol, 9.94; 4-fluorophenol, 9.80; 2,4-difluorophenol, 8.58; 2,3,6-trifluorophenol, 6.73; 2,3,4,6-tetrafluorophenol, 5.96; and pentafluorophenol, 5.83. Thus, proton abstraction may be expected to be slightly exothermic for the most acidic chemical (pentafluorophenol), endothermic for phenol, and between these two extremes of -26 and 160 kJ mole^{-1} for all other fluorinated phenols.

In this work, the pathway from the association product to a proton abstracted ion was explored as a function of pK_a of the ArO–H bond. In this manner, the rules governing proton abstraction versus association might be delineated for these and other chemicals with mildly acidic hydrogens. A set of fluorinated benzyl alcohols was employed as controls or analogs to the phenols where the methylene unit –CH_2– served to electronically isolate the O–H bond from the electronic effects from the aromatic ring. In addition, the thermal stabilities of association products, $M \cdot Cl^-$, were explored using ion mobility spectrometry (IMS) where interface region artifacts could be avoided and ions could be considered thermalized.

Ion mobility spectrometry is an instrumental method suited for the characterization of organic and inorganic compounds based upon ion mobility or size-to-charge ratio rather than mass-to-charge ratio [20]. In IMS, substances are ionized via APCI reactions and ions are characterized at ambient pressure in a drift tube culminating with a mobility spectrum (a plot of detector current versus time of drift). In studies of gas phase ion chemistry at ambient pressure by IMS, various reversible reactions may form a mixture of product ions in the ion source region. However, ions are extracted from the ion source region into a clean and dry gas environment devoid of sample neutrals and all forward reactions cease; thereafter, only ion decomposition [21] or declustering [22] occur. When the kinetics of this decomposition are slow, such reactions appear as distortion from a Gaussian peak shape in the ion mobility spectrum and can be used to determine the rate of dissociation and the heat of interaction [22]. As such, an IMS can permit studies of ion behavior using thermalized ions without complications of APCI-MS where supersonic expansion may distort ion distributions. In the experiments described below, the goal was to explore, by APCI-MS, the rules that govern negative ion formation and to examine, by IMS, the thermal instability of ions created through association reactions.

Experimental

Atmospheric Pressure Chemical Ionization/Tandem Mass Spectrometer

A TAGA 6000 APCI-tandem mass spectrometer (MS/MS) from Sciex, Inc. (Toronto, Ontario, Canada) was equipped with a corona discharge ion source, API Standard Software, Ver 2.5.1 (PE SCIEX), and Apple PowerMac 7100/66 computer. An all glass sampling train with three access ports for sample, reagent gas, and clean nitrogen was used for sample delivery to the corona discharge ion source of the TAGA. A detailed description of this triple quadrupole has been given [23] and operating conditions are given in Table 1. Lens potentials were initially optimized for ion intensity using reagent ions from air; later only the orifice potential was varied to control ion energies for the fluorinated phenol product ions.

Ion Mobility Spectrometer

An ion mobility spectrometer was built to operate from 25 to 250 °C with nitrogen drift gas at ambient pressure. Details of this instrument are given in Table 1. The drift gas was pre-purified nitrogen purchased from Argyle

Table 1. Dimensions and operating parameters of APCI-triple quadrupole mass spectrometer and high temperature IMS drift tube

APCI-Triple Quadrupole Mass Spectrometer

Discharge current (μA)	3	L5 (V)	250
Needle to plane distance (cm)	0.5	L6 (V)	−40
Discharge plate potential (kV)	0.6	R1 or Q1 (V)	−40
Discharge current (μA)	3	R2 or Q2 (V)	0
Orifice (OR) potential (V)	−60	R3 or Q3 (V)	−40
L2 (V)	−53	Base vacuum (torr)	3×10^{-6}
L3 (V)	−45	Collision gas pressure (torr)	2×10^{-5}
L4 (V)	−40		

Ion Mobility Spectrometer

Length of drift region (cm)	5.2	Length of ion source region (cm)	1.3
Insulator ring inner diameter (cm)	1.9	Amount of ^{63}Ni in source (mCi)	10
Insulator ring outer diameter (cm)	5.1	Electric field in drift region (V/cm)	250
Insulator ring thickness (cm)	1	Frequency of shutter pulse (Hz)	40
Conducting ring inner diameter (cm)	1.9	Drift gas (air) flow rate (ml/min)	200
Conducting ring outer diameter (cm)	4	Temperature of drift gas (°C) (preheated)	25–200
Conducting ring thickness (cm)	0.2	Delay in spectra (ms)	2
Shutter diameter (mm)	13	Shutter pulse (μs)	100
Collector diameter (mm)	9.5	No. of points digitized per spectrum	640
Aperture diameter (mm)	10.3	Collector-aperture voltage (V)	100
Detector aperture distance (mm)	~1	No. of averages per spectrum	32

Insulating rings: high temperature Teflon.
Conducting rings: 303 stainless steel.
Shutters and detector were obtained from a CAM instrument and used without modification.

Welding Company (Las Cruces, NM). In order to avoid excessive clustering between ions and water from the purified nitrogen, gas was passed through a 1.4 m long × 8 cm ID moisture scrubber containing 5× molecular sieve and activated charcoal. Resulting moisture in the scrubbed nitrogen was 2–10 ppm and was monitored using a MS2 Panametric Moisture Meter (Waltham, MA). The nitrogen gas was passed into the IMS drift tube at a constant rate of 200 ml min^{-1} during the experiment. A reagent gas, carbon tetrachloride, was generated from a thermostated diffusion source created from a 1-dram minivial with a cap supporting a 15 mm long 1.0 mm ID glass tube. This was held in a Kintek glass container (Houston, TX) that was placed in an aluminum block (45 °C) and controlled with a digital heater (model CT137, Minco Inc., Minneapolis, MN) at 40 °C. The loss of CCl$_4$ vapors in the gas flow of the drift tube was gravimetrically determined as 1.5 μg s^{-1} yielding, after dilution with the drift gas flow, a net vapor concentration of 281 ng ml^{-1} in the ion source. Signal was collected using digital signal averaging with a analog-to-digital conversion board (Graseby Ionics Inc. Watford, UK) located in an Intel 80286-based computer.

Vapor Generator

A vapor generator, designed and built at Varian Associates, Inc. (Palo Alto, CA), was used to create a vapor stream of sample. The generator has been described in detail [24]. Vapor samples were gravimetrically assayed using an AD-6 microbalance (Perkin Elmer Corporation, Norwich, CT) located on a vibration-arrest plat-

form (Eberbach Corp., Ann Arbor, MI). Pre-purified and scrubbed nitrogen was provided at a rate of 80 ml min^{-1}.

Chemicals

All chemicals were obtained commercially and used without purification. Suppliers included Aldrich Chemical Company (Milwaukee, WI) for phenol, 4-fluorophenol, 2,4-difluorophenol, 2,3,6-tri-fluorophenol, pentafluorophenol, benzyl alcohol, 4-fluorobenzyl alcohol, 2,4-difluorobenzyl alcohol, 2,3,6-trifluorobenzyl alcohol, and pentafluorobenzyl alcohol and Lancaster Chemical Co. (Windham, NH) for 2,3,5,6-tetrafluorophenol.

Chemical Purity

Each chemical was screened by HPLC with a 254-nm UV detector, a gas chromatograph with flame ionization detector, and by GC/MS and all samples were found to have >99.5% purity. Minor impurities did not contain functional groups anticipated to interfere with APCI reaction chemistry and were not deemed significant.

APCI-MS and MS/MS Studies

Several separate studies were made where mass spectra were collected for each chemical under various experimental conditions as described below. In each of these, the method of introducing sample and reagent gas was common throughout. Reagent chemical and sample were placed into separate containers attached to the

glass sample train. Scrubbed nitrogen gas was added to the last port of the train at 5–10 psig at ~8.6 l min^{-1}. The nitrogen flow, in combination with suction applied to the ionization chamber of the TAGA 6000 (throttled to a low flow sufficient only to clear the source region of nitrogen feed gas), caused reagent chemical and sample to be volatilized and transported into the corona discharge source. This method of sample delivery provided a controlled atmosphere free of ambient air impurities. In practice, background spectra (i.e., no sample) were obtained first to insure cleanliness in the ion source and the sampling train. Then sample was added to the remaining port and measurements were commenced.

1. Single mass spectra: In this study, MS conditions per Table 1 were used with Q2 and Q3 in rf-only modes and mass spectra were obtained using Q1. Scan ranges were from 10 amu to a value greater than that of $M_2 \cdot Cl^-$ for individual chemicals.
2. Interface studies: The potential differences in the interface region of the APCI-MS can cause collision activated dissociation and might alter ratios of $(M - H)^-$ versus $M \cdot Cl^-$ ions in the supersonic expansion region. The orifice potential was set at 3 V intervals from −73 to −53.5 V with the first lens set to −53 V and spectra were obtained each potential step for each chemical at room temperature in nitrogen.
3. Nitrogen as supporting gas: Spectra of individual chemicals were obtained using procedures described in (1) with nitrogen alone as the reagent gas. Consequently, there were no reagent ions such as O_2^- or Cl^- for the formation of adduct ions.
4. MS/MS experiments: CID studies of $M \cdot Cl^-$ for each chemical were made to determine branching ratios as a function of ion energy. The potential for the orifice was −60 V and the potential on Q1 was −40 V; Q2 was set to voltages of −5, −2, 0, 2, 5, and 10 V and daughter ion spectra were obtained from the $M \cdot Cl^-$ ion. The scan range in Q3 was 10 amu to slightly above the adduct ion m/z.
5. Influence of CCl_4 reagent gas concentration: Four concentrations of carbon tetrachloride were studied and included extremes between no CCl_4 and vapor saturation. The gas phase concentrations of CCl_4 for these were determined gravimetrically as 0, 116, 930, and 5820 μg ml^{-1}. The fluorophenols were generated from a diffusion source and concentrations were calculated using known mass flux rates at room temperature. Vapor levels for chemical were not allowed to saturate the ion source region and a residual intensity for the reactant ion peak was always present during all experimental conditions listed in Table 1.
6. Repeatability: Five replicate spectra were obtained for pentafluorophenol under conditions given for single mass spectral scan as described above in (1) and for trifluorophenol using CID studies as described in (4).

Ion Mobility Spectrometry Studies

Each chemical was screened using the IMS at a given temperature for the vapor generator and the IMS drift tube. The general procedure involved inserting a pre-sized glass NMR tube (10 cm long × 4 mm ID × 5 mm OD) containing 0.5 ml or 50–100 mg of a chemical into the vapor generator. This was accomplished by removing the access cap to the generator body, placing the tube into the heated chamber, and replacing the stopper to the access port. Next, mobility spectra were acquired and stored continuously until the intensity of the product ions became constant, usually with some residual intensity for the reactant ions. This was assessed by viewing the spectra over a period of 2 min and by comparing the relative peak heights of the product ions in each acquisition. After the acquisition, the tube was removed from the vapor generator and a period of at least 10 min was used to allow the IMS and vapor generator to clean before the introduction of the next sample. Mass flux rates (ng s^{-1}) for chemicals were: 63, phenol; 134, 4-fluorophenol; 446, 2,4-difluorophenol; 272, 2,3,6-tri-fluorophenol; 500, pentafluorophenol; 47, benzyl alcohol; 64, 4-fluorobenzyl alcohol; 200, 2,4-difluorobenzyl alcohol; 43, 2,3,6-trifluorobenzyl alcohol; and 56, pentafluorobenzyl alcohol. Concentrations can be calculated using the total flow rates of vapor generator and drift gas (280 ml min^{-1}) to yield concentrations of 9–107 ng ml^{-1}. Reduced mobilities (K_o) for the chloride ion and other ions were calculated using trinitrotoluene as a reference chemical. Values for K_o for Cl^- were dramatically affected by temperature and ranged from 1.3 to 3.2 cm^2 V^{-1} cm^{-1} at 25–200 °C, respectively.

At elevated temperatures for the drift tube (100–250 °C), the effects of changes in sample vapor concentrations were measured by controlling the temperature of the vapor generator (25–90 °C in increments of 10 °C). Effects from concentration changes of sample were minor and predictable; thereafter, vapor concentrations for samples were kept constant as studies on drift tube temperature were continued from 100 to 25 °C.

Results and Discussion

APCI-mass Spectrometry of Fluorinated Phenols and Benzyl Alcohols

Mass spectra from APCI-MS characterization of phenol, fluorophenol, and difluorophenol (in nitrogen) with Cl^- as a reagent ion yielded the adduct ion $M \cdot Cl^-$ (Figure 1a–c) at m/z values of 129, 147, and 165, respectively. The identification was supported further by the 3:1 ratio of $^{35}Cl^-$:$^{37}Cl^-$ as expected for a chloride adduct ion. The presence of residual reactant ions of Cl^-, $H_2O \cdot Cl^-$, and $(H_2O)_2 \cdot Cl^-$ at m/z 35, 53, and 71, respectively, are pronounced in Figure 1a,b and were routinely used to insure cleanliness of the source region and freedom from O_2^- arising from intrusion of air into the TAGA ionization region. As anticipated for APCI reactions
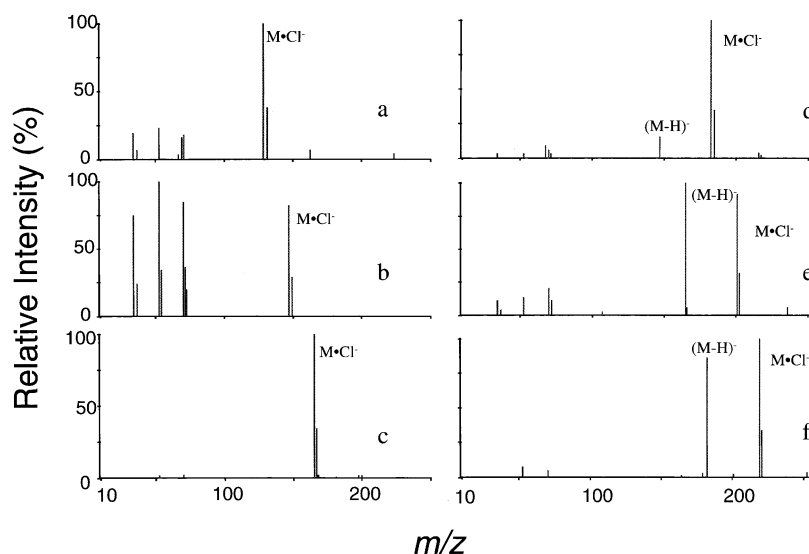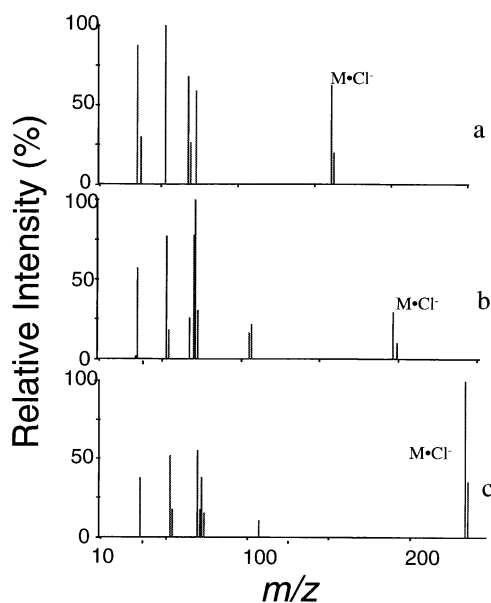
Figure 1. Mass spectra from atmospheric pressure chemical ionization of phenol and fluorophenols in nitrogen with Cl^- reagent ion. Chemicals were (**a**) phenol, (**b**) 4-fluorophenol, (**c**) 2,4-difluorophenol, (**d**) 2,3,6-trifluorophenol, (**e**) 2,3,5,6-tetrafluorophenol, and (**f**) pentafluorophenol.

where fragmentation is virtually nil, no other product ions were detected, except the occasional and minor presence of $M_2 \cdot Cl^-$ (not shown).

Mass spectra for tri, tetra-, and pentafluorophenols (Figure 1d–f) exhibited a second product ion, $(M - H)^-$, which arose through proton abstraction reactions, presumably as shown in eq 6. Substitution by fluorines is known to increase the gas phase acidity of the O–H bond in PhO–H and proton abstraction was anticipated for the highly fluorinated phenols. Intensity for the

abstracted ion for tetra- and pentafluorophenol was virtually equal to the intensity for $M \cdot Cl^-$ and suggests that roughly half of the total amount of the adduct ions was converted to $(M - H)^-$. Proton abstraction with trifluorophenol was only at ~20% intensity relative to $M \cdot Cl^-$ and this was expected where acidity was low compared to that of pentafluorophenol. The proton abstraction step (eq 6) certainly follows the initial step of adduct formation (eq 5), but the APCI-MS results did not prove if the proton abstraction was occurring in the ion source region or in the energetic interface region of the TAGA where collision induced dissociations (CID) are known to occur [22]. This can be controlled somewhat with potentials between the orifice and lens but

Figure 2. Mass spectra from atmospheric pressure chemical ionization of benzyl alcohol and fluorobenzyl alcohols in nitrogen with Cl^- reagent ion. Chemicals were (**a**) 4-fluorobenzyl alcohol, (**b**) 2,3,6-trifluorobenzyl alcohol, and (**c**) pentafluorobenzyl alcohol.
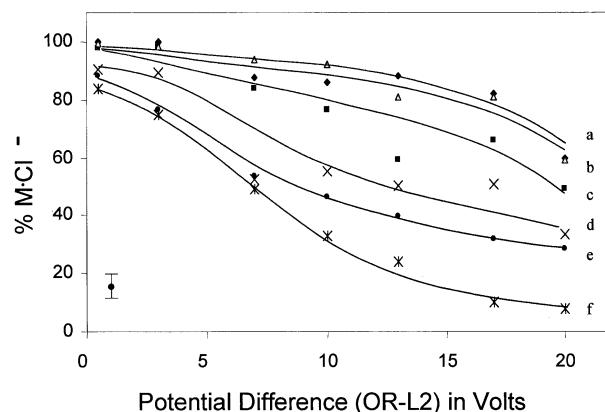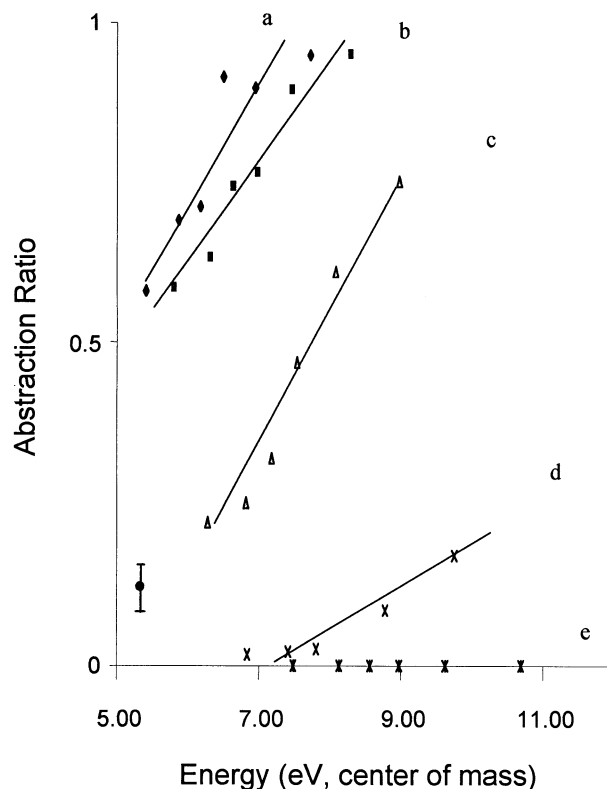

Figure 3. Relative abundance of $M \cdot Cl^-$ in APCI-MS of fluorophenols for potentials between the orifice and the first lens (L2) in the interface region. The chemicals were (**a**) phenol, (**b**) fluorophenol, (**c**) difluorophenol, (**d**) trifluorophenol, (**e**) pentafluorophenol, and (**f**) tetrafluorophenol. Abundances were normalized to total product ion intensity. Note error bar for reproducibility.
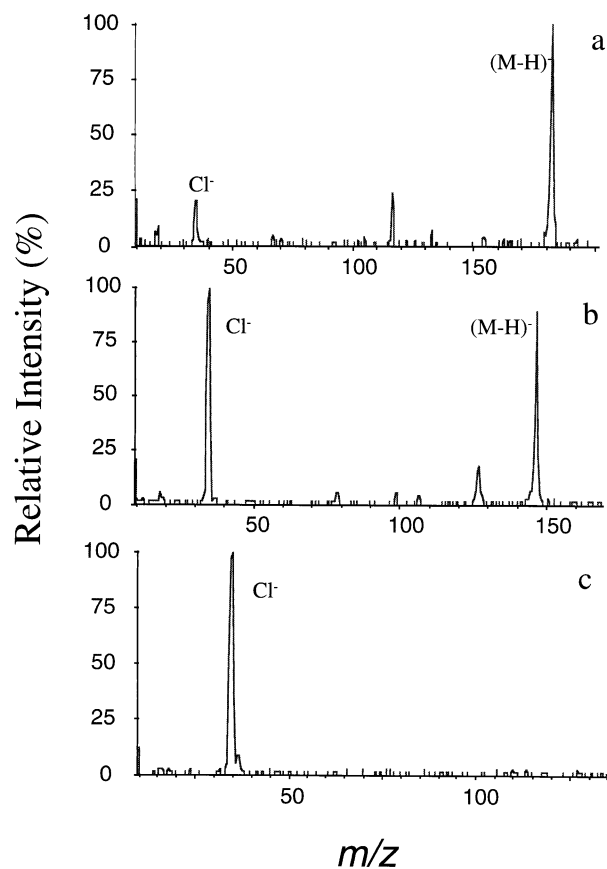
Figure 4. Daughter ion spectra from CID experiments using M · Cl⁻ for (**a**) pentafluorophenol, (**b**) trifluorophenol, and (**c**) phenol. The ion energies were ~10 eV (center of mass).

Figure 5. Effect of ion energy on proton abstraction ratio ($I_{(M-H)^-}/I_{(M-H)-} + I_{M\cdot Cl}^-$) in CID experiment with M · Cl⁻ for phenols and fluorophenols. Chemicals were (**a**) pentafluorophenol, (**b**) tetrafluorophenol, (**c**) trifluorophenol, (**d**) difluorophenol, and (**e**) fluorophenol.

mass spectra alone did not disclose if the proton abstraction was occurring readily in the corona discharge or arising as a result of passing through the MS interface, i.e., an artifact of the measurement in APCI-MS as described in the next section.

Other control experiments were made and included chemical controls, study of the effect of reagent gas concentration, repeatability of ion abundances, and use of only nitrogen gas in the ionization source. The chemical controls, i.e., benzyl alcohol and fluorinated benzyl alcohols, were used to probe the influence on acidity from ring versus side chain substitutions since the methylene group of the ØCH₂O–H bond should insulate the O–H bond from ring substitutions. Mass spectra for several fluorobenzyl alcohols are shown in Figure 2 and fluorine substitution had no influence on the product ion identity which was in all cases M · Cl⁻. This suggests that the acidity of the O–H in fluorinated phenols bond was indeed affected by degree of ring substitution by fluorine and that the proton abstraction could be associated with acidity. The influence of reagent gas concentration was not statistically different from the repeatability which was roughly ±5%–10% on peak heights. Finally, electron attachment in nitrogen with any of the chemicals was very weak to nil.

Proton Abstraction and the Vacuum Interface Region

Passage of the adduct ion M · Cl⁻ through the vacuum interface is known to add energy to ions sufficient to cause CID and potentially also proton abstraction. This energy can be controlled through potential differences on the orifice and first lens (L2) and has been used for CID studies [25]. The results shown in Figure 3 demonstrate that the ratio of (M − H)⁻ to M · Cl⁻ was also influenced by the OR and L2 potentials and, consequently, some amount of the proton abstractions seen in Figure 1 had been occurring in the interface region. At small potential differences (OR-L2 of 0.1–3 V), the principal ion for all phenols was the adduct. Some proton abstraction is seen for the tri-, tetra-, and pentafluorophenol even at the lowest setting of 0.5 V and as a result the experiment did not conclusively demonstrate where proton abstraction was occurring: in the ion source region or in the vacuum interface region. Moreover, the presence of some dimer adduct ion intensity and residual Cl⁻ intensity from the reagent ions complicated calculations on the ratio of adduct ion versus proton abstracted ion. As a consequence, the results in Figure 3 provide only experimental guidelines for subsequent studies and disclosed no unequivocal measure of ion energetics. Nonetheless, the results demonstrate that energy placed into
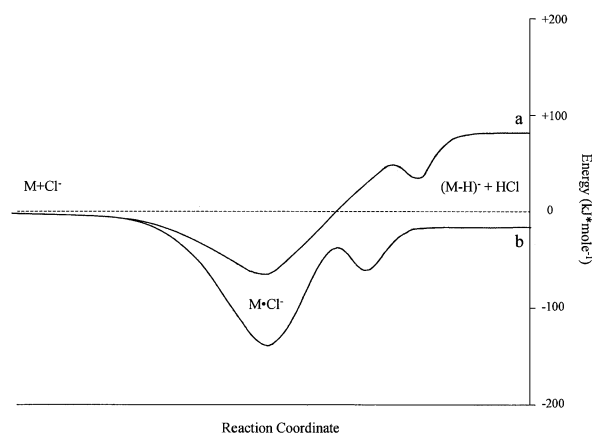
Figure 6. Reaction profile for proton abstraction in APCI-MS or IMS measurements. The first step is the formation of a stable M · Cl$^-$ intermediate which can be converted to the abstracted product (M − H)$^-$ with addition of energy.

M · Cl$^-$, for any of the fluorophenols including phenol, could cause proton abstraction reactions. All further studies were made using potential differences of 5–10 V for OR-L2, thus providing intensities of M · Cl$^-$ sufficient for CID experiments.

Collision Induced Dissociation of M · Cl$^-$ in Q2

When M · Cl$^-$ was isolated and subjected to CID with Ar in Q2, two pathways for dissociation were observed: simple decomposition to M and Cl$^-$ and proton abstraction to (M − H)$^-$ and HCl. These two ions are seen in Q3 scans for CID of penta-, tri-, and monofluorophenol Cl$^-$ adducts in Figure 4 for an ion energy of ~10 eV (center-of-mass). The pentafluorophenol · Cl$^-$ adducts (Figure 4a) underwent principally proton abstraction as expected for an acidic proton (pK_a = 5.83) and yielded only minor amounts of Cl$^-$. In contrast, M · Cl$^-$ for monofluorophenol (pK_a = 9.94) exhibited no proton abstraction and only simple dissociation at this ion energy (Figure 4c). The product ion spectrum for M · Cl$^-$ of trifluorophenol showed a nearly equal distribution between (M − H)$^-$ and Cl$^-$ as expected for a fluorophenol with acidity (pK_a = 6.73) between the extremes of phenol and pentafluorophenol (Figure 4b). A third CID product was observed for the tri- to pentafluorinated phenol · Cl$^-$ adducts at m/z of 117 and 129. These most probably arise from eliminations of C_2FO and water from the (M − H)$^-$ ions, respectively, and were seen only at comparatively high energies.

The influence of ion energy on extent of proton abstraction from the adduct ion in CID experiments is shown in Figure 5 where increases in ion energy promoted the proton abstraction reaction for all chemicals except phenol (not shown) and also fluorophenol, for which no measurable proton abstraction occurred between 7 and 13 eV. The influence on the proton abstraction from degree of fluorine substitution followed the trend expected from solution acidities [23], namely:

pentafluorophenol > tetrafluorophenol

> trifluorophenol > difluorophenol;

monofluorophenol and phenol = no abstraction

In summary, these results demonstrate that the proton abstracted ion (M − H)$^-$ could be created directly from the adduct ion when provided with sufficient energy and the extent of proton abstraction was controllable by the ion energies. Also, the extent of proton abstraction was governed by the anticipated gas phase acidity of the O–H bond as influenced by ring substitutions with fluorine. These findings support the following reaction coordinate shown in Figure 6 where the molecule association with the Cl$^-$ is exothermic and leads to a stable M · Cl$^-$. Proton abstraction for either phenol · Cl$^-$ (a) or pentafluorophenol · Cl$^-$ (b) will be endothermic and should pass through a transition state as shown in Figure 6. The results also suggested that energy necessary to abstract a proton from chloride adducts of tetra- and pentafluorophenol is comparatively low but removal of a proton from the M · Cl$^-$ adduct for phenol and fluorophenol is strongly endothermic. This suggests that the proton abstraction occurred in the vacuum interface region of the APCI-MS and not in the ion source; however, this conclusion is based upon indirect rather than direct measurements and the use of another method for ion characterization was needed. Ion mobility spectrometry (IMS) provides a means of studying ions under thermalized conditions and can provide a measure of ion behavior without interfaces or expansion regions to distort ion energies. In addition, chemical events that occur on the millisecond time scale, such as ion declustering or ion fragmentation, can be observed directly [25] in IMS.

Thermalized Ions in Ion Mobility Spectrometry

Mobility spectra for phenol and trifluorophenol are shown in Figure 7 with Cl$^-$ as the reagent ion in nitrogen drift gas. The mobility spectra for phenol (Figure 7a) showed residual intensity of the reactant ion (Cl$^-$) and product ions at 10 ms (50 °C) consisting of both M · Cl$^-$ and M · O$_2^-$ (revealing a small air impurity in the nitrogen gas or entering the ionization region). Nonetheless, the two product ions were partly resolved and the K_0 values for these ions matched those from mass identified mobility spectra. Neither mobility spectrum at 50 or 100 °C showed evidence for the formation of an (M − H)$^-$ arising from proton abstraction. At temperatures above 100 °C, the adduct ion M · Cl$^-$ was decomposed to Cl$^-$ and at 150 °C, the M · Cl$^-$ was thoroughly decomposed to Cl$^-$ only. No proton abstraction to (M − H)$^-$ was observed. Comparable patterns in spectra with the same temperatures were obtained for mono- and difluorophenol, suggesting common behavior of M · Cl$^-$ ions.

The mobility spectrum for trifluorophenol (Figure
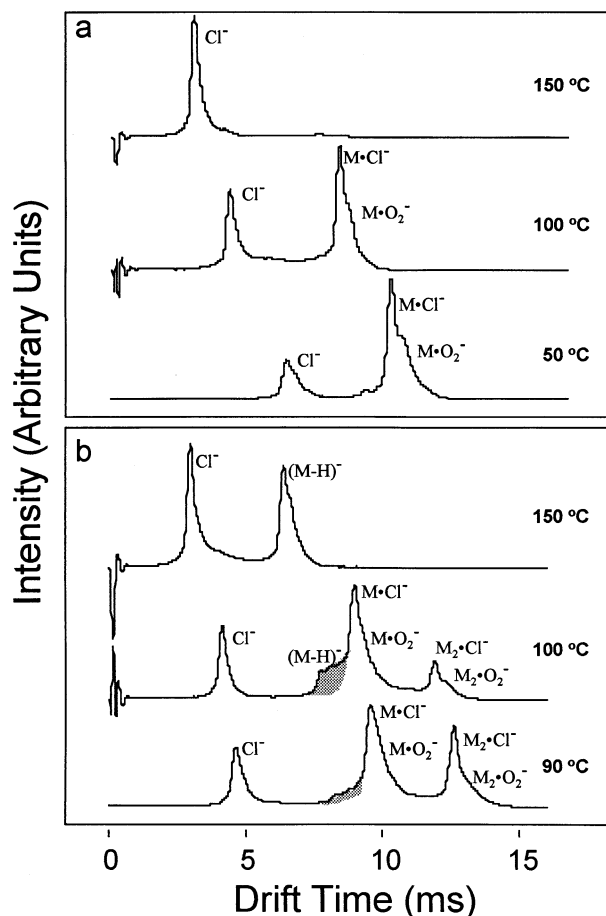
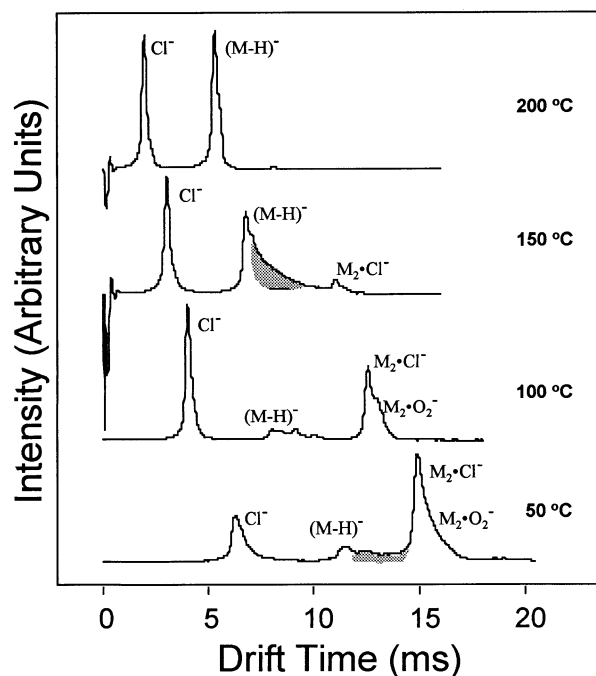**Figure 7.** Mobility spectra for phenol (**a**) and trifluorophenol (**b**) in nitrogen with Cl⁻ reagent ion.

Figure 8. Mobility spectra for pentafluorophenol in nitrogen with Cl⁻ reagent ion at temperatures from 50 to 200 °C.

7b) showed residual intensity of Cl^- and both $M \cdot Cl^-$ and $M_2 \cdot Cl^-$. A slight distortion at the leading edge of the adduct ion (see shaded region of mobility spectrum at 90 °C) was observed and can be attributed to drift tube reactions of the adduct ion to an ion with higher mobility than the adduct, namely, the proton abstracted ion $(M - H)^-$. This suggests that $(M - H)^-$ was arising directly from the decomposition of $M \cdot Cl^-$ in the drift region of the mobility spectrometer and that decomposition occurs on a time scale near that of ion drift (7–9 ms). At 100 °C, this was evident in the comparatively large shaded region where $M \cdot Cl^-$ was undergoing conversion to $(M - H)^-$. At 150 °C, the only ion observed was the $(M - H)^-$ from the proton abstraction reaction. These results confirm generally the reaction profile where an adduct ion is a stable intermediate which can undergo proton abstraction if provided sufficient energy.

Mobility spectra for pentafluorophenol are shown in Figure 8 and illustrate that the tendency toward proton abstraction was more pronounced for pentafluorophenol than for trifluorophenol. A pronounced $M_2 \cdot Cl^-$ was observed at 50 °C and was consistent with APCI-MS measurements and there was the suggestion

of a small amount of $(M - H)^-$ and a slight elevation in the baseline (shaded region from 7 to 9 ms) indicating the reactions of $M_2 \cdot Cl^-$ to $(M - H)^-$ in the drift region. At 100 °C, a sharp increase in Cl^- was observed with a loss in dimer adduct ion intensity and the dimer adduct ion was nearly eliminated at 150 °C. The predominant product ion at 150 °C was an $(M - H)^-$ with a broad tail. This is evidence that $(M - H)^-$ was being formed from $M_2 \cdot Cl^-$ directly or perhaps through $M \cdot Cl^-$. Certainly, adduct ions for pentafluorophenol and Cl^- were totally abstracted by 200 °C. This was consistent with the results from CID inside the interface region where ion energies should be expected to be greater than those in the Q2 CID studies.

The drift times or K_0 values for each ion were characteristic of ion identity in the mobility spectra and patterns of K_0 values for each chemical from 50 to 200 °C are shown in Figure 9. Mobility spectra for phenol and fluorinated phenols (Figure 9a) showed three distinct ion groups which included the $(M - H)^-$, $M \cdot Cl^-$, and $M_2 \cdot Cl^-$ and these are shown as shaded regions. There is a spread in K_0 values for a given ion throughout the range in temperature since the ion identities are $(H_2O)_n \cdot M \cdot Cl^-$ and n is a function of temperature. Hydration is pronounced at low temperatures (i.e., K_0 values are smaller at low temperature than those for the same chemical at high temperature). These were loosely held and did not survive transit through the dry plenum gas of the APCI-MS and were not observed in mass spectra. The results in Figure 9a summarize the findings from the IMS studies and illustrate that proton abstracted ions were observed in the IMS studies, regardless of temperature, only for tri-,
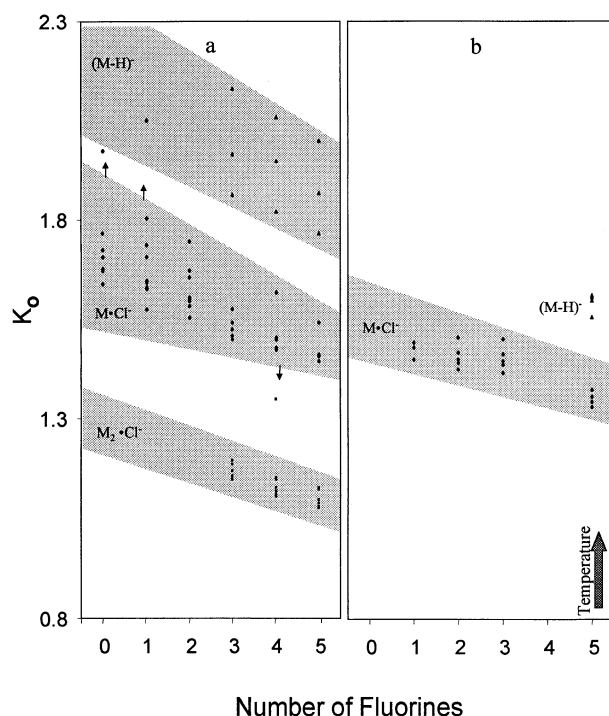
Figure 9. Reduced mobilities for ions from mobility spectra for (**a**) phenol and fluorinated phenols and (**b**) benzyl alcohol and fluorinated benzyl alcohols throughout the temperature range of 50–200 °C (note arrow). The shaded regions show (from bottom to top) ions of $M_2 \cdot Cl^-$, $M \cdot Cl^-$, and $(M - H)^-$ and are arranged according to the number of fluorine substitutions on the aromatic ring.

tetra-, and pentafluorophenol. The adduct ion, $M \cdot Cl^-$, existed for all chemicals but $(M - H)^-$ could not be created from for thermalized ions from phenol, mono-, and di-fluorophenols at any temperature. Hence, the shaded zone shows that no $(M - H)^-$ ions were observed. The behavior for benzyl alcohol and fluorinated benzyl alcohols mirrored that of phenol and showed only the $M \cdot Cl^-$. The appearance of a second ion in the mobility spectra for pentafluorobenzyl alcohol was not mass identified and is unknown pending IMS/MS studies.

Conclusions

Proton abstractions for fluorinated phenols occurred through a stable intermediate adduct ion, $M \cdot Cl^-$, when provided sufficient energy either through potential differences in a mass spectrometer or through thermal energy in an ion mobility spectrometer. The reaction may be seen as an elimination of HCl from the adduct ion, $M \cdot Cl^-$. The degree of fluorine substitution on the ring clearly affected the tendency of a molecule to undergo proton abstraction from the adduct ion and followed calculated solution acidities for the O–H bond. Acidic fluorinated phenols exhibited proton abstraction to a degree greater by far than phenol or monofluorophenol which have smaller acidities. These findings suggest that in instances where acidic protons exist on a

molecule in the range of aqueous phase pK_a values of 5.8–6.7 or smaller, product ions from proton abstraction should be anticipated in ion mobility spectrometry at elevated temperatures or from interface artifacts in APCI-mass spectrometry.

Acknowledgments

References

1. Dzidic, I.; Carroll, D. I.; Stillwell, R. N.; Horning, E. C. *J. Amer. Chem. Soc.* **1974**, *96*, 5258.
2. Dzidic, I.; Carroll, D. I.; Stillwell, R. N.; Horning, E. C. *Anal. Chem.* **1975**, *47*, 1308.
3. Thenot, J.-P. *J. Chromatogr.* **1977**, *142*, 481.
4. Karasek, F. W. *Anal. Chem.* **1971**, *43*(14), 1982.
5. Karasek, F. W.; Tatone, O. S. *Anal. Chem.* **1972**, *44*(11), 1758.
6. Karasek, F. W.; Tatone, O. S.; Kane, D. M. *Anal. Chem.* **1973**, *45*(7), 1210.
7. Blyth, D. A. "The Detection of Mustard Agent Vapour using Ion Mobility Techniques (U)," Technical Paper No. 264, Chemical Defence Establishment, Porton Down, Salibury, Wilts, England, January 1980, ADB047586.
8. Fetteroff, D. D.; Clark, T. D. *J. Forensic Sci.* **1993**, *38*(1), 28.
9. Danylewych-May, L. L.; Cumming, C. In *Advances in Analysis and Detection of Explosives*; Yinon, J., Ed.; 1993, p 385.
10. Karasek, F. W.; Spangler, G. E. In *Electron Capture—Theory and Practice in Chromatography*; Zlatkis, A.; Poole, C. F., Eds.; Elsevier: Amsterdam, 1981, pp 384–406.
11. Horning, E. C.; Carroll, D. I.; Dzidic, I.; Stillwell, R. N. In *Electron Capture—Theory and Practice in Chromatography*; Zlatkis, A.; Poole, C. F., Eds.; Elsevier: Amsterdam, 1981, pp 359–374.
12. Harrison, A. G. *Chemical Ionization Mass Spectrometry*; CRC: Boca Raton, FL, 1983, pp 22–29.
13. Protor, C. J.; Todd, J. F. J. *Organ. Mass Spectrom.* **1983**, *18*, 509.
14. Lawrence, A. H.; Neudorfl, P. *Anal. Chem.* **1988**, *60*, 104.
15. Spangler, G. E.; Lawless, P. A. *Anal. Chem.* **1978**, *50*, 884.
16. Smith, G. B.; Eiceman, G. A.; Walsh, M. K.; Critz, S. A.; Andazola, E.; Ortega, E.; Cadena, F. *Field Anal. Chem. Tech.* **1997**, *1*(4), 213.
17. NIST Standard Reference Database Number 69, November 1998 Release.
18. Deturi, V. F.; Ervin, K. M. *Int. J. Mass Spectrom. Ion Processes* **1998**, *175*, 1.
19. Pearce, P. J.; Simkins, R. J. J. *Can. J. Chem.* **1968**, *46*, 241.
20. Eiceman, G. A.; Karpas, Z. *Ion Mobility Spectrometry*; CRC Press: Boca Raton, FL, 1994.
21. Eiceman, G. A.; Shoff, D. B.; Harden, C. S.; Snyder, A. P. *Int. J. Mass Spectrom. Ion Processes* **1988**, *85*, 265.
22. Ewing, R. G. *Kinetic Decomposition of Proton Bound Dimer Ions with Substituted Amines*, Ph.D. Dissertation; New Mexico State University: Las Cruces, NM, 1996.
23. Dawson, P. H.; French, J. B.; Buckley, J. A.; Douglas, D. J.; Simmons, D. *Organ. Mass Spectrom.* **1982**, *17*, 205.
24. Eiceman, G. A.; Preston, D.; Tiano, G.; Rodriguez, J.; Parmeter, J. E. *Talanta* **1997**, *45*, 57–74.
25. Wensing, M. W.; Snyder, A. P.; Harden, C. S. *Rapid Commun. Mass Spectrom.* **1996**, *10*, 1259.